EXPERIMENTS AND MODELING OF CLAMPING EFFECTS ON THE BEARING STRENGTH OF MECHANICALLY FASTENED JOINT IN CFRP LAMINATES

F.-X. Irisarri[a*], T. Vandellos[a], P. Paulmier[a], F. Laurin[a]

[a]*Onera – The French Aerospace Lab, F-92322 Châtillon, Cedex*
**francois-xavier.irisarri@onera.fr*

Keywords: bolted joint, bearing strength, clamping.

Abstract

In the present study, an experimental investigation has been performed on 16-ply carbon/epoxy T700GC/M21 laminates. Three stacking sequences have been tested with pin-loading conditions and bolted conditions with increasing clamping force. Progressive damage and failure in clamped specimens were examined using acoustic emission and load-displacement measurement. Evolution of the clamping force during loading was also monitored. Experimental results show significant influence of clamping on bearing damage and failure of the laminates with an increase of the first peak bearing load of about 100% for the finger-tight specimens. Higher clamping pressure resulted in a slight further increase of the first peak bearing load. Numerical study will follow.

1. Introduction

Due to their high specific strength and stiffness, Carbon Fibre-Reinforced Plastics (CFRP) have been increasingly used in aeronautical applications these last decades. These applications require the use of mechanical joints in order to transfer loads between composite components and other composite or metallic parts. Since the use of bonded joints is often prohibited by the industrial imperatives of reproducibility and maintenance, mechanically fastened joints are preferentially used. However, CFRP components can be considerably weakened by the introduction of holes, mostly because of high stress concentrations. The resulting mechanisms of local progressive degradation lead to three main competing failure modes (focusing on the composite element of the joint), namely tension, shear and bearing. Optimal design of composite joints usually leads to a competition between tensile and bearing failure. Both failure modes have been the focus of significant research efforts in the past [1-3]. Geometrical effects and stacking sequence effects on these failure modes are now well understood and can be captured by advanced modeling techniques [4]. However, to our knowledge, no model has been published up to now that can capture the effects of the clamping force on the bearing strength of bolted joints in composite laminates.

In the present study, an experimental investigation has been performed on 16-ply carbon/epoxy T700GC/M21 laminates. Three stacking sequences have been tested with pin-loading conditions and bolted conditions with increasing clamping force. Progressive damage and failure in clamped specimens were examined using acoustic emission and load-displacement measurement. Evolution of the clamping force during loading was also monitored. The experimental results presented in this paper form the first part of a larger study that will involve FE modeling and progressive damage simulation in a second part.

This paper focuses on the experimental results. Section 2 presents the specimen and the test set-ups. The experimental results are presented and discussed in Section 3.

2. Specimen and experimental set-ups

Three 16-ply laminates are studied here. The laminate configurations are detailed in Table 1. A quasi-isotropic laminate (hereafter named QI) is used as reference configuration as it is known to be a very configuration to sustain high bearing stress. This reference laminate is compared against a quasi-isotropic laminate (named QId) containing a 45/-45 interface and a 0/90 interface. These interfaces are both prone to delamination due to high Poisson ratio mismatch. This stacking order is expected to reduce the bearing strength of the laminate. A third configuration is studied that presents more plies in 90°- direction than in 0°-direction and also contains weak interfaces with respect to delamination. This last configuration is expected to present the lowest bearing strength.

Laminate	**Stacking sequence**	**Type**
QI	$[(-45/90/45/0)_2]_s$	Quasi-isotropic
QId	$[-45/90/45/-45/0/0/90/45]_s$	Quasi-isotropic prone to delamination
OR	$[-45/45/90/0/90/90/45/-45]_s$	Orientated (90°-dominated)

Table 1. Laminate configurations.

The laminates were manufactured from T700GC/M21 carbon/epoxy prepreg sheets using a hot-press. The specimens were machined from 300 mm × 300 mm plates to the geometry shown in Figure 1. Nominal dimensions are D = 6.35 mm for the pin diameter, w = 36 mm for the width, e = 30 mm for the end distance and L = 135 mm for the total length of the specimen. The theoretical thickness of the specimen is t = 4.16 mm. The dimensions were specified in order to obtain bearing failure in the laminates. All tests were run in displacement control at a rate of 10^{-5} m/s. The gripping area length is about 50 mm for all tests.

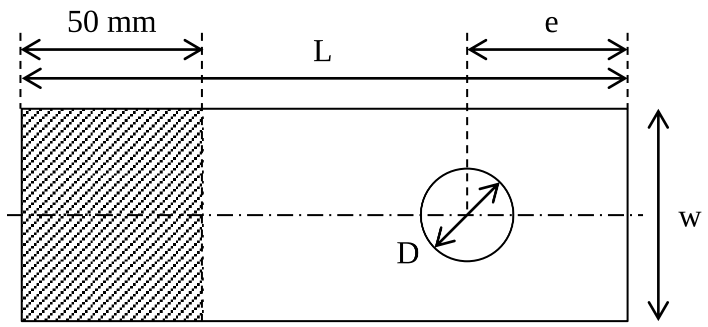

Figure 1. Dimensions of the specimen.

2.1. Specimen and experimental set-up for pin-loaded bearing tests

The experimental set-up for the pin loading test is shown in Figure 2. The specimen is loaded through a hardened steel pin. The specimen is loaded in tension. The loading direction corresponds to the direction of the fibers in the 0°-plies. An apertured flange is designed to enable observation of the surface of the specimen in front of the pin, in the loading direction, using digital image correlation (DIC). Acoustic emission (AE) was used to monitor the development of damage during the tests. Load and displacement measurement were obtained using the test machine captor.

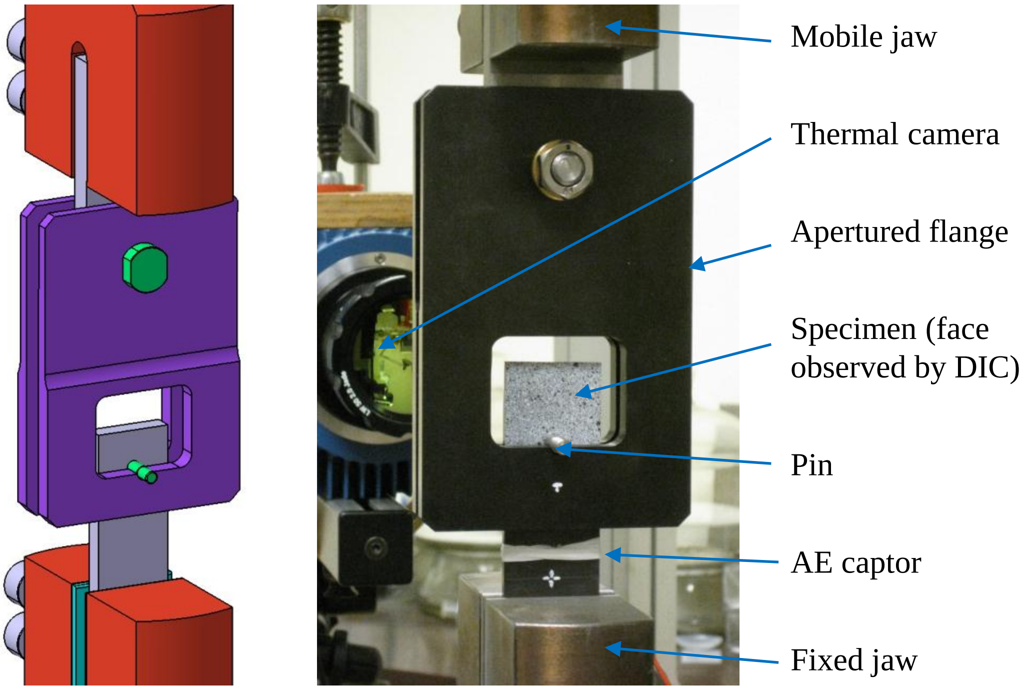

Figure 2. Experimental setup for the pin-loaded bearing tests.

Measured dimensions of the specimen are detailed in Table 2. Hole internal diameter could not be measured was sufficient accuracy in this study, thus the specified tolerances are given instead. Clearance between the hole and the fastener, defined as the difference between the diameters, varies between 30 µm and 60 µm.

Specimen ID	**Specimen dimensions**				**Fastening system**		**Clamping load [kN]**
	***w* [mm]**	***L* [mm]**	***t* [mm]**	***D* [mm]**	**D_p [mm]**	**D_w [mm]**	
QI-M11	36.02	134.93	4.11			-	-
QI-M13	36.02	134.94	4.17			-	-
QI-M14	36.02	135.01	4.20	6.35 +0.03 / 0	6.32	-	-
OR-M1	36.03	134.84	4.09			-	-
QId-M1	36.02	134.85	4.08			-	-

Table 2. Specimen configurations for pin-loaded bearing tests.

2.2. Specimen and experimental set-up for bolt-loaded bearing tests

The experimental set-up for the bolt loaded test is shown in Figure 3. Due to the clamping system, observation of the surface of the laminate near the hole could not be performed. Instrumentation consists of acoustic emission and load and machine displacement. Additionally, the fastener is instrumented with a load cell that enables to monitor the evolution of the clamping force during the test.

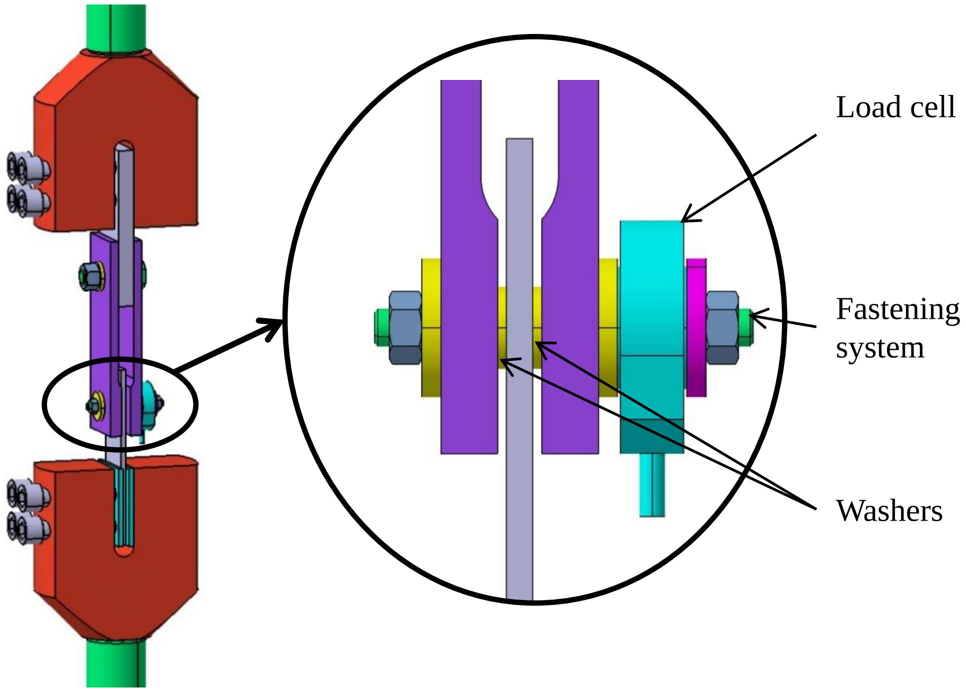

Figure 3. Experimental setup for the bolt-loaded bearing tests.

Several initial clamping forces were imposed to assess the influence of clamping on the bearing behavior of the laminates. Additionally, a 13 mm diameter washer and a 16 diameter washer were used to assess the influence of the area of the clamping surface on bearing. The inner diameter of the washers D_{wi} is 6.4 mm and 6.5 mm respectively. Measured dimensions of the specimen and initial clamping forces are detailed in Table 3.

Specimen ID	Specimen dimensions				Fastening system		Clamping load [kN]
	w [mm]	*L* [mm]	*t* [mm]	*D* [mm]	D_p [mm]	D_{we} [mm]	
QI-M3	36.02	135.00	4.18		6.32	13.00	0.5
QI-M17	36.02	134.99	4.16		6.32	13.00	5.5
OR-M5	36.03	134.81	4.19		6.33	13.00	0.5
OR-M6	36.03	134.85	4.19		6.33	13.00	5.0
OR-M7	36.03	134.86	4.17		6.33	13.00	0.5
OR-M8	36.03	134.95	4.15	6.35	6.33	13.00	9.6
OR-M9	36.03	134.80	4.13	+0.03 / 0	6.33	16.00	0.5
QId-M5	36.02	134.85	4.20		6.33	13.00	0.5
QId-M6	36.02	134.97	4.20		6.33	13.00	5.0
QId-M7	36.02	134.94	4.19		6.33	13.00	0.1
QId-M8	36.02	134.96	4.17		6.33	13,00	9,6
QId-M9	36.02	134.60	4.15		6.33	16.00	0.5

Table 3. Specimen configurations and initial clamping forces for bolt-loaded tests.

3. Experimental results

The experimental results are presented in Table 4. Pin-loaded tests are used as reference results to assess the effect of clamping on the bearing strength of the specimens. Bearing strength is defined here as the bearing stress at the first peak bearing load. Bearing stress is defined as follows:

$$\sigma_b = F/(D\times t), \quad (1)$$

where F represents the applied bearing load, D is the hole diameter and t the thickness of the laminate. The percentage of improvement in bearing strength due to clamping is indicated between brackets in the Table 4. The reference test (QI laminate in pin-bearing) was repeated three times and showed very little dispersion. Dispersion was not studied for other configurations but is assumed to be low.

The results show very high improvement in static bearing strength for the lowest clamping forces (finger tight). Constraining the laminate to prevent normal expansion of the damaged material on the loaded side of the hole is enough to nearly double the bearing strength with the washer of exterior diameter 13 mm. The 16 mm washer results in an even higher increase. For the OR and QId laminate the increase in strength is approximately proportional to the increase of the diameter of the washer for finger tight configurations.

Further increase in clamping load increases the strength but with a much slower rate: between finger tight configurations and 10 kN clamping force (about 100 MPa clamping stress), the additional strength increase is about 20 % and seems to evolve rather linearly with respect to the clamping force.

Specimen ID	Clamping load [kN]	Washer D_{we} [mm]	Section D×t [mm²]	First peak load [kN]	Bearing strength [MPa]
QI-M11	-	-	25.98	13.30	512
QI-M13	-	-	26.35	13.61	516
QI-M14	-	-	26.54	13.65	514
QI-M3	0.08	13.00	26.46	25.07	947 (+84 %)
QI-M17	5.69	13.00	26.29	25.29	962 (+87 %)
OR-M1	-	-	25.85	11.28	436
OR-M7	0.09	13.00	26.40	22.35	847 (+94 %)
OR-M5	0.51	13.00	26.52	21.58	814 (+87 %)
OR-M6	5.18	13.00	26.52	23.80	898 (+106 %)
OR-M8	9.99	13.00	26.27	25.25	961 (+120 %)
OR-M9	0.13	16.00	26.14	24.55	939 (+115 %)
QId-M1	-	-	25.79	11.19	434
QId-M7	0.10	13.00	26.52	25.10	947 (+118 %)
QId-M5	0.54	13.00	26.59	24.24	911 (+110 %)
QId-M6	5.20	13.00	26.59	25.72	967 (+123 %)
QId-M8	9.98	13.00	26.40	27.54	1043 (+140 %)
QId-M9	0.09	16.00	26.30	27.40	1042 (+140 %)

Table 4. Experimental results.

Laminates do not benefit from clamping to the same extend. Laminates prone to delamination (QId and OR) benefits the most from clamping. Indeed, the lateral constraint prevents the delamination from opening as long as they are confined under the washers. Figure 4 shows the evolution of the static bearing strength of the laminates as a function of the clamping stress. The clamping stress is supposed to be uniform over the area confined by the washers and is defined as follows:

$$\sigma_c = 4 \times F_c / [\pi \times (D_{we}^2 - D_{wi}^2)], \tag{2}$$

where F_c represents the initial clamping force measured before applying any bearing loading to the specimens. It is interesting to see in the figure the bearing strength of the clamped QId specimens is comparable to the strength of the clamped QI specimens at equivalent clamping stress although the strength of the pinned QId specimen is 15 % lower than the pinned QI laminate. Clamping prevents the delamination from opening under the washers thus limiting the effect of the stacking order of the plies. The OR laminate presents similar evolution of the bearing strength with the clamping stress, but the bearing strength remains lower than the one of the QI laminates because of the reduced proportion of 0°-plies.

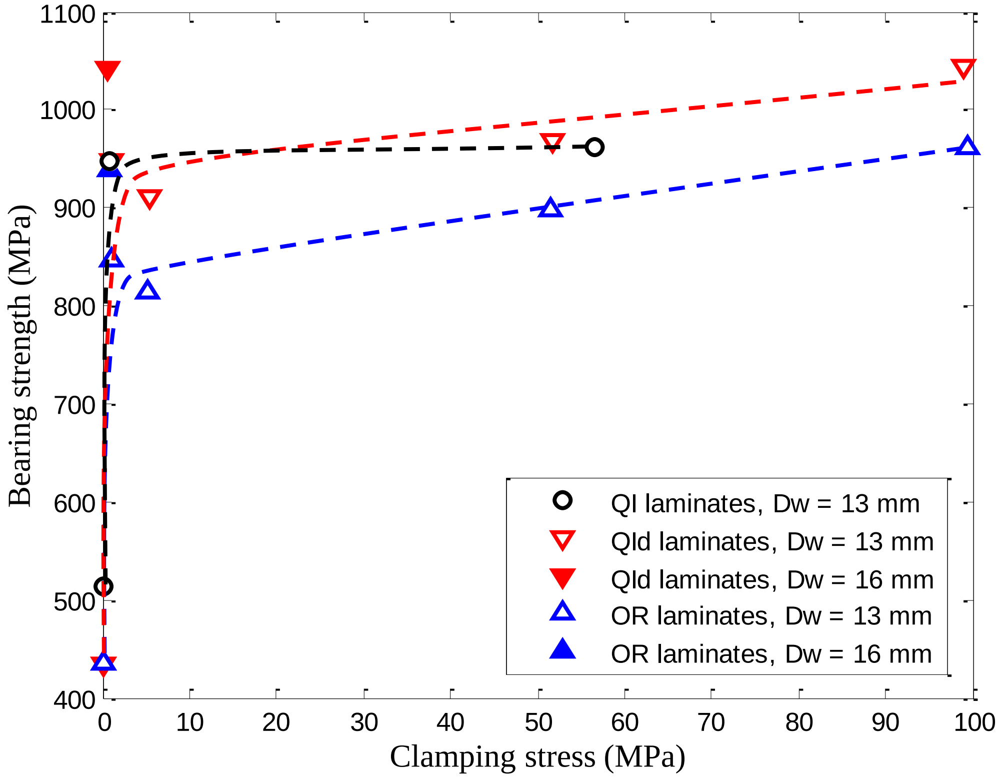

Figure 4. Evolution of the bearing strength with respect to the clamping stress for three laminates.

Figure 5 shows the influence of the lateral constraint on the behavior of the joint. The displacement measured by the machine are consistent between the tests and show no significant influence of the test set-up (pin-bearing or bolt-bearing) and the value of the clamping force on the global stiffness of the joint. On the contrary, the stacking sequence has a perceptible influence on the stiffness of the joint and varies here with the proportion of 0°-plies, i.e. the QI and QId specimens present equivalent joint stiffness, slightly higher than the OR specimens.

The tests were stopped before the final failure of the specimens, excepted for the specimens with the largest washer (QId-M9 and OR-M9) that failed in tensile mode after significant bearing damage. The first peak bearing was usually the highest load monitored, expected for the clamped QI specimen (QI-M3 and QI-M17) that were stopped shortly before the load reached 30 kN, which was fixed as the limit not to damage the fastener.

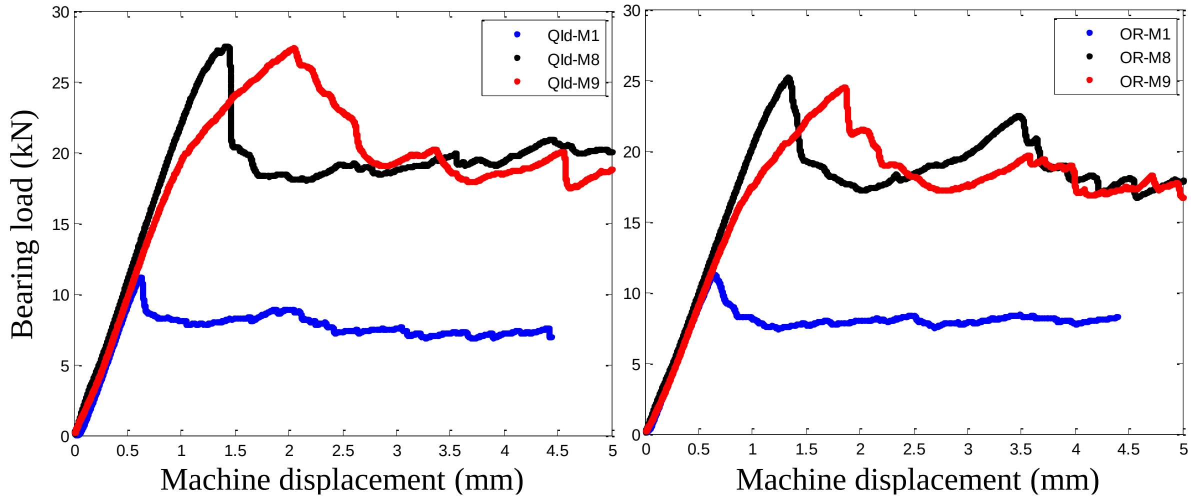

Figure 5. Comparison between the pin-loaded and the bolt-loaded bearing behaviors.

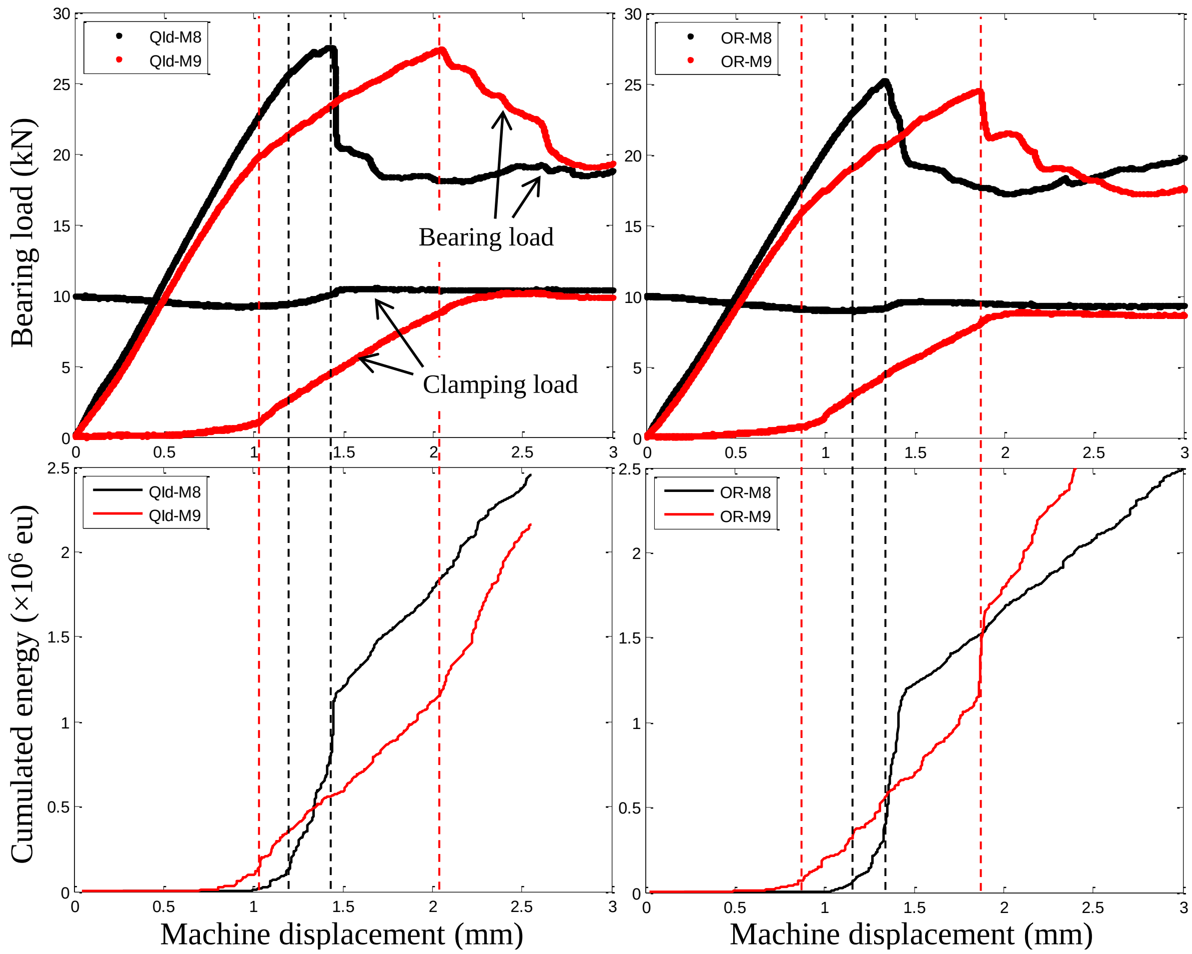

Figure 6. Compared evolutions of the clamping force and the cumulated energy of acoustic events.

The bearing behavior of the clamped QId and OR specimen is plotted in Figure 6 together with the evolution of the cumulated energy of the measured acoustic events. The acoustic emission curve gives information about the evolution of damage during loading. For each laminate, the two specimens compared present similar bearing strength. However they correspond to very different fastening conditions. For specimens M8 the clamping force is 10 kN with a 13 mm diameter washer. For specimens M9 the clamping force is 100 N with a 16 mm diameter washer. In the case with the highest clamping force, the behavior is approximately linear with no acoustic event monitored until a first significant damage event that occurs at about 90 % of the bearing failure load. The clamping load decreases slightly in this first phase of the test because of Poisson effects. After this point, damages quickly accumulate under the washers until the bearing failure load that is associated to a second major acoustic event. This second phase of the test is quite short. The corresponding part of the bearing curve is nonlinear. The clamping force increases during this phase of local damage accumulation. After the peak bearing load, damage propagates outside the area constrained by the washer, with large scale instable delamination and fiber kinking in the 0°-plies. The clamping load remains stable. In the case of the finger-tight specimens, the same phases are observed during the tests. Nevertheless, the damage accumulation phase starts earlier and lasts much longer before bearing failure occurs.

4. Conclusions and future work

The experimental results presented in this paper show two interesting points about the influence of the clamping force on the bearing strength of the laminate. The first point is the spectacular and already well documented increase in bearing strength due to clamping. In particular, clamping prevents the opening of delamination under the washers, thus limiting the effect of the stacking order of the plies, although very significant in pin-loaded configuration. The second point is the combined influence of the size of the washer and the clamping load on the damage accumulation phase prior to the first peak bearing load.

In the second part of this study, these results are analyzed using finite element analysis and progressive failure modeling. The Onera Progressive Failure Model (OPFM) [5] is used to capture the effects of fiber failure and inter-fiber failure on the behavior of the ply. Two approaches are compared to model interlaminar damages. The first approach is based on the use of cohesive zone models inserted between the plies. Delamination is described as a surface damage. By contrast, in the second approach, delamination is handled with a diffuse continuum damage approach in the volume of the plies. The method consists in adding to the OPFM approach an interlaminar damage variable. Effects of delamination are captured through degradation of the out-of-plane properties of the plies. The numerical results are compared with experimental data to assess their capacity to capture the effect of clamping on the bearing strength of the laminates. In particular hydrostatic pressure effects on the intra-laminar damage in the vicinity of the bolt and effect of the normal stress on delamination are investigated.

References

[1] T. A. Collings. The Strength of Bolted Joints in Multi-Directional CFRP Laminates. *Composites* 8(1):43-55, 1977.

[2] G. Kelly and S. Hallström. Bearing strength of carbon fibre/epoxy laminates: effects of bolt-hole clearance. *Composites: Part B* 35:331-343, 2004.

[3] P. A. Smith and K. J. Pascoe. The effect of stacking sequence on the bearing strengths of quasi-isotropic composite joints. *Composite Structures* 1986 (6):1–20, 1986.

[4] P. P. Camanho and L. Tong. *Composite joints and connections*. Woodhead Publishing, 2011.

[5] F. Laurin, N. Carrere, C. Huchette, J.-F. Maire. A multiscale hybrid damage and failure approach for strength predictions of composite structures, *Journal of Composite Materials*, 47 (20-21):2713-2747, 2013.